JOURNAL OF CATALYSIS 67, 331–347 (1981)

The Relationship of Structure and Activity of NiMo Sulfides to Composition of the Precursor Oxides

J. V. SANDERS AND K. C. PRATT

CSIRO Division of Materials Science, University of Melbourne, Parkville, Victoria 3052, Australia

Received May 5, 1980; revised July 23, 1980

Mixed oxides of Ni and Mo formed from coprecipitated powders with a variety of compositions from pure MoO_3 to pure NiO have been examined by X-ray diffraction and electron microscopy before and after their conversion to sulfides and use as a hydrodesulfurization (HDS) catalyst. The Mo-rich oxides are a mixture of MoO_3 and $NiMoO_4$. Sulfiding transforms the MoO_3 into MoO_2 crystals coated with a thin skin of MoS_2, together with some flakes of MoS_2; the $NiMoO_4$ transforms to highly dispersed MoS_2. In Ni-rich samples, Mo up to at least 30% cannot be detected directly in the electron microscope but is thought to be incorporated within the NiO, producing disorder within the crystals. Conversion of this material produces crystals of nickel sulfides of various compositions, coated with a layer of MoS_2. Electron micrographs of the most active catalysts contain sets of black fringes with a 6.15-Å spacing taken to be lattice images of layers of MoS_2. Nickel is homogeneously associated with this highly dispersed MoS_2, but is not resolvable by electron microscopy.

1. INTRODUCTION

Molybdenum-based catalysts used for hydrodesulfurizing (HDS) reactions are promoted by the addition of cobalt or nickel in much more than trace amounts (*1*). A number of possible mechanisms for the activation of MoS_2 by cobalt (nickel) have been proposed. These rely on suggestions of edge intercalation of the promoter (*2, 3*); a degree of synergy between the sulfides of Mo and Co (Ni) (*4, 5*); the semiconducting nature of the catalyst (*6*); or the distribution of the active sulfides as a monolayer on the surface of the support (*7, 8*). Possible structural arrangements have been based mainly on X-ray diffraction evidence (*9, 10*) or scanning electron microscopy (*11*).

In order to obtain more information about the structures of catalysts in this system, we have examined by high-resolution transmission electron microscopy the structures of both the precursor mixed oxides, and the sulfides formed from them. In the first instance we have chosen the Ni–Mo system, and examined a set of unsupported catalyst samples. The mixed oxides were made by coprecipitation over a wide range of compositions (*12*). Different Ni/Mo ratios were obtained by controlling the concentrations and flow rates of the two mixing solutions.

Specimens were examined before and after sulfiding, and tested for activity by the hydrogenolysis of thiophene. The specimens were examined by X-ray powder diffraction (XRD) to characterize the average crystalline composition, and selected-area electron diffraction was used to identify components of mixtures seen in the electron microscope. In this way we have been able to understand the extent to which the structure of the active catalyst is controlled by the structure and morphology of the oxide mixture from which it was formed.

2. EXPERIMENTAL

A set of nine binary oxide samples at roughly equal composition intervals from

0021-9517/81/020331-17$02.00/0

pure NiO to pure MoO_3 was made by coprecipitation of solids which were then converted to oxides by heating at 673 K for 4 hr. Details of the technique have been described by Pratt *et al.* (*13*). This process was adopted here in order to simulate in a reasonably close manner the standard commercial practice for the preparation of supported catalysts of this type. However, it is difficult in the first instance to make mixtures of precisely predetermined composition. Therefore, the actual compositions were obtained by chemical analyses of the powders after their preparation and use. For this reason the intervals of composition between the various samples (Table 1) are not quite equal.

About 0.5 g of each sample was treated with a 20% H_2S/H_2 stream in a catalytic reactor, and used for hydrogenolyzing thiophene at 595 K for typically 8 hr. Details and results of these tests are given by Pratt *et al.* (*13*).

Samples were stored under N_2 until required for electron microscopy; the powder was then dispersed ultrasonically in ethyl alcohol and a small amount of the suspension collected on a holey carbon film on an electron microscope grid. They were examined in a JEOL 100 CX fitted with an UHR pole piece (C_s = 0.7 mm) and used in the top-entry configuration.

Individual features or crystalline components of specimens were identified by selected-area electron diffraction in the conventional manner. The smallest area which could be isolated in this way was about 0.7 μm in diameter.

X-Ray diffraction, using Cu or Co radiation, was carried out in a Siemens D500 diffractometer on dry powder compressed into a slot 0.5 × 0.2 × 20 mm in an aluminum plate.

3. RESULTS

3.1. The Oxides

Table 1 lists the compositions, color, and crystalline components identified from XRD powder patterns of the samples of Ni–Mo oxides used. The samples will be consistently identified by the letters A–J. We describe below the morphology and structures of these mixed oxides as shown by electron microscopy, and subsequently described the sulfides in a similar way.

The crystalline components of the powders, determined from X-ray and electron diffraction, are presented in Fig. 1a for the oxides, and in Fig. 1b for the sulfides. These composition diagrams are schematic only and we do not imply that they contain quantitative information about the relative amounts of the phases present in the catalysts.

TABLE 1

Composition, Structure, and Color of Binary Oxide Samples

Sample	Composition Ni/Ni + Mo (atom%)	Color	Structure, X-ray and electron diffraction
A	0	White	MoO_3
B	30	Gray-green	MoO_3 + $NiMoO_4$
C	41	Green	MoO_3 + $NiMoO_4$
D	55	Gold	$NiMoO_4$ + tr. NiO
E	73	Brown	NiO
F	79	Black	NiO
G	92	Black	NiO
H	99.8	Black	NiO
J	100	Black	NiO

FIG. 1. Schematic composition diagrams of the crystalline components found by X-ray and electron diffraction of the binary Ni–Mo system: (a) oxides; (b) sulfides used as catalysts.

3.1.1. 100% Mo

The oxide was MoO_3, in the form of angular crystals without any regular shape, 0.1–1 μm in average dimension (Fig. 2).

3.1.2. Mo + 30%–50% Ni

Two separate phases MoO_3 and $NiMoO_4$ were identified from XRD patterns. No significant line broadening occurred.

There were four distinct morphological components in the electron micrographs; their phase was identified by electron diffraction.

(i) MoO_3 occurred as large crystals, mostly regularly shaped as laths terminated crystallographically at one end like a picket. Typically, they had a length/width ratio of 5 or more, with lengths 1–7 μm and widths 0.2–1 μm. An example is shown in Fig. 3, where the large crystal dominating the field is MoO_3, and the other small crystals are all $NiMoO_4$ in various forms.

(ii) $NiMoO_4$ occurred as crystals with three distinct shapes generally mixed in various proportions. They are all shown in the electron micrograph in Fig. 4 as P, N, or C. The crystals P are holey plates, often fan-shaped, about 2 μm wide; N are needles of irregular thickness and not crystallographically terminated; C are individual

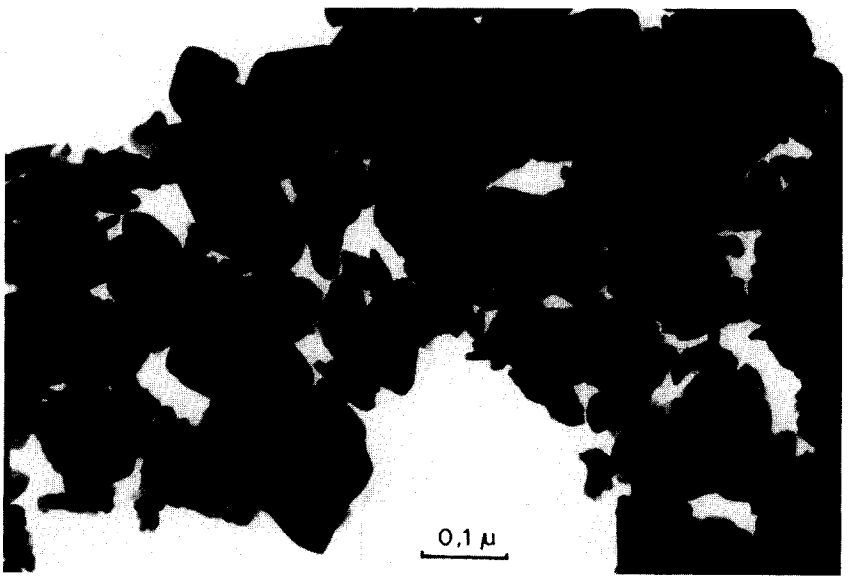

FIG. 2. Electron micrograph of sample A, showing the MoO_3 crystals produced by calcining the precipitate.

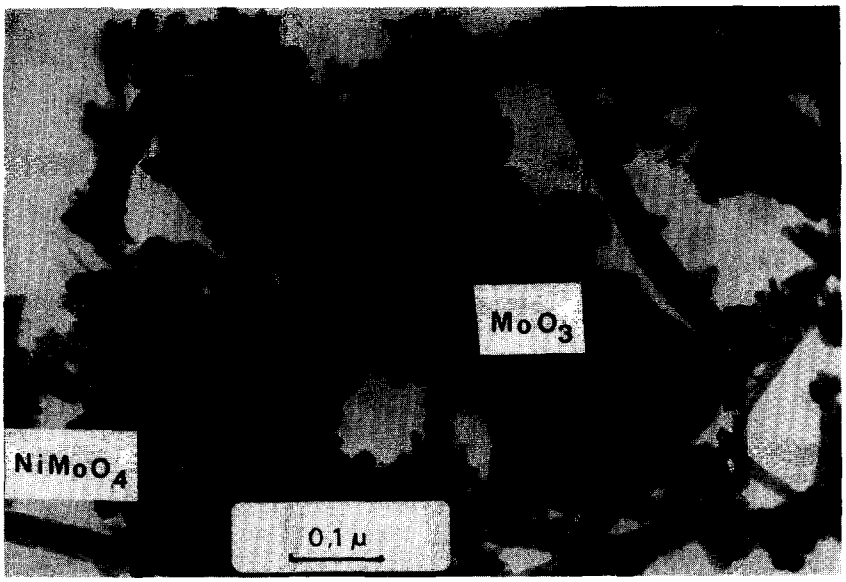

FIG. 3. Electron micrograph of sample C, 41% Ni, showing a large crystal of MoO_3 among a variety of smaller crystals of $NiMoO_4$ in various shapes.

small crystals 100–200 Å in size, clustered together and mixed with, but not attached to, the needles. Figure 4 is from sample C; in sample B, containing a lower nickel content, the needles were larger, but otherwise the mixture was much the same.

3.1.3. Mo + 50% Ni

With the technique of coprecipitation it is not easy to make mixtures of exactly predetermined composition. The mixture closest to this composition was sample D, which

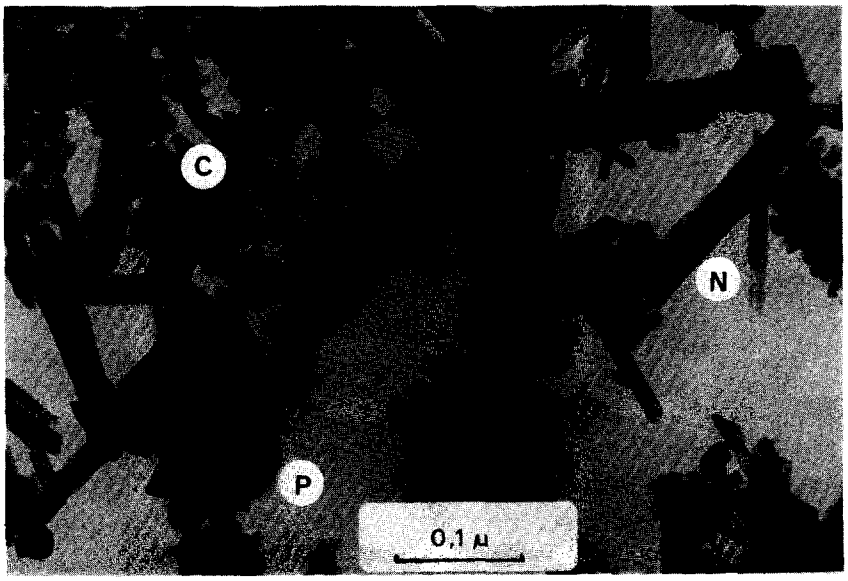

FIG. 4. Electron micrograph of sample C; all the crystals are $NiMoO_4$ but they may be as plates (P), needles (N), or small individual crystals (C).

was found to be slightly richer in Ni than 50%. It consisted predominantly of a homogeneous distribution of plates of $NiMoO_4$, irregular in shape and thickness, and could best be described as a collection of small angular crystals joined together in the same orientation (Fig. 5). There were also small amounts of a separate phase, NiO, in a highly dispersed form; it probably comes from the excess of Ni above the 50%. This material is similar to NiO identified in the next section (3.1.4).

The X-ray pattern from this sample indexed convincingly as $NiMoO_4$ (*14*) but contained one extra weak line at $d = 3.336$ Å, which could indicate the presence of a small amount of the "N phase" reported to occur in this composition range (*15*). This pattern fits reasonably well to that of a hydrated $NiMoO_4$ given in ASTM 12-348.

3.1.4. Mo + 50–100% Ni

The only crystalline phase detected in this region was NiO; the morphology was homogeneous within each sample.

Pure NiO (sample J) consisted of plates exposing (111) faces, containing holes. They were roughly hexagonal in shape, but not uniform in thickness (Fig. 6). The crystal dimensions were about $0.2 \times 0.2 \times 0.01$ μm. The edges of the crystals and holes within them tended to be in [110] directions.

The addition of Mo produced disorder within these plates, the extent of this disorder increasing with the Mo concentration, so that at the highest Mo content in the range (specimen E, 27% Mo) the effective crystal size as measured by the broadening of the XRD powder lines was only about 40 Å. This effect is shown in Table 2 where the crystal size shown was calculated from the

TABLE 2

X-Ray Line Broadening for NiO Samples

Sample	Composition (atom%Ni)	Broadening		Crystal size (Scherrer) (Å)
		37°	43.5°	
E	74	2.5°	3°	38
F	77	2.3°	2.9°	37
G	92	1.5°	1.8°	76
H	99.8	0.7°	0.9°	214
J	100	0.3°	0.2°	300

FIG. 5. Electron micrograph of the binary oxide of nearly equal amounts of Ni and Mo in sample D, shows the homogeneous crystallinity of the $NiMoO_4$.

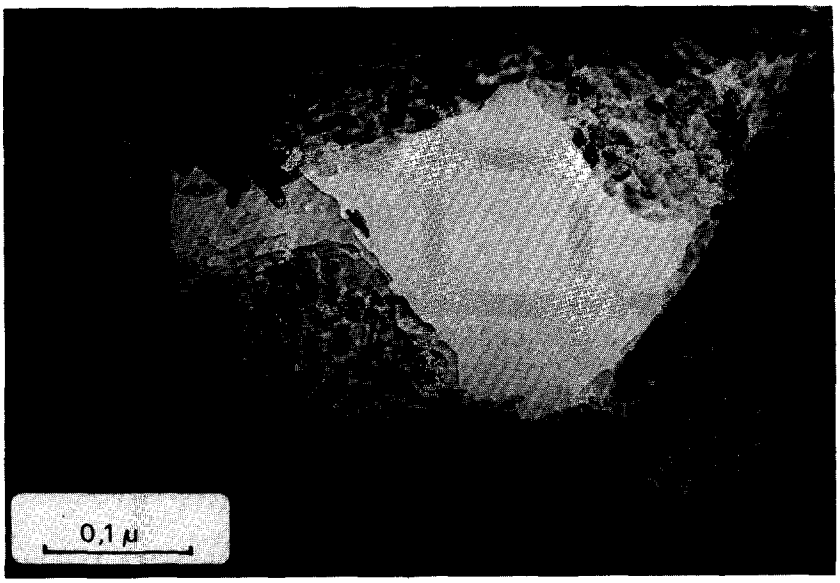

FIG. 6. Electron micrograph of NiO crystals in sample J, 100% Ni, showing that they form thin, holey hexagonal plates, some of which can be seen edge-on at the left-hand side.

X-ray linewidth at half-height using the simple Scherrer formula. No crystals of $NiMoO_4$, nor any oxide of molybdenum were found in this range. There was no change in crystal structure or morphology of specimen E (27% Mo) when it was heated for 4 hr at 500°C.

The effect of incorporating a small amount of Mo into the precipitate is best shown in dark-field electron microscopy on the sample H (0.2% Mo). The oxide plates still retain the form of crystals of pure NiO, but there is strain contrast within the plates (Fig. 7). A dark-field image of such a plate (Fig. 7b) contains bright domains several hundred angstroms in extent, the bright areas being made up of sets of fringes of spacing from 3 to 100 Å, but roughly parallel (± 10°) over the plate. It can be shown by analysis of diffraction conditions that these are rotational Moiré fringes. Thus each bright area in the dark-field picture represents at least two overlapping plates, with a relative rotation of a few degrees between them. The spacing of the Moiré fringes and the extent of arcing in electron diffraction patterns show that for specimen H the rotation is typically 20–30°. With increasing Mo concentration, the size of the domains decreases and the extent of the angular disorder increases, until with specimen E (27% Mo), the original morphology of the NiO plates can only just be detected, and the effective crystal size is only about 40 Å.

It is possible that Mo is soluble in the NiO crystals, in which case we could expect the lattice parameter of the NiO to be modified. Therefore we took an accurate step-scan X-ray trace from specimen E (27% Mo) over the 111 and 200 peaks (from 2θ = 35° to 47.25°, CuKα radiation). The unusually heavy background made the 111 peak unsuitable for such a measurement, but the 200 peak gave a value a = 4.169 Å, which is 0.2% different from the accepted value, a = 4.177 (*16*). This difference is hardly significant for such a broad line (1.85° half-width, giving a crystal size of 50 Å), so we conclude that there is no evidence for dissolution of Mo in the NiO.

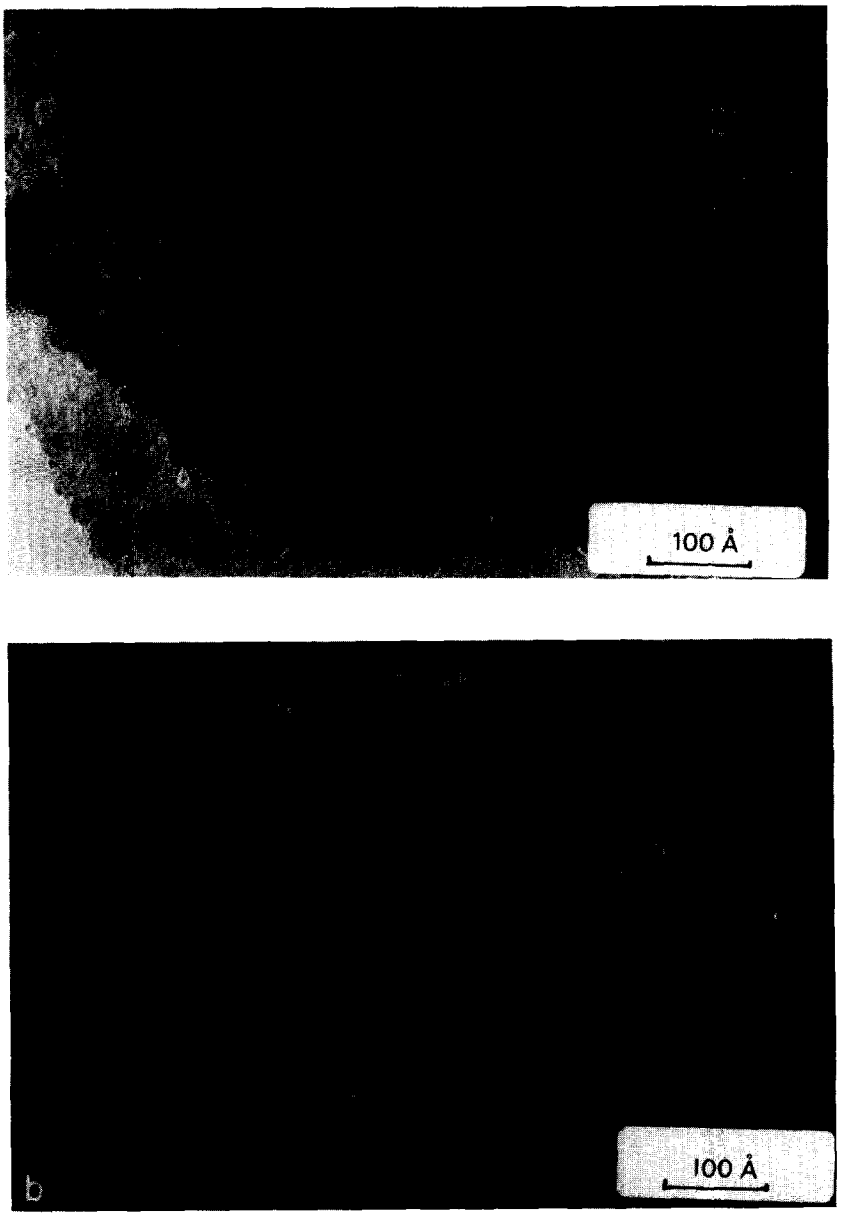

FIG. 7. Disorder introduced into a crystal of NiO by the coprecipitation of 0.2% Mo, is shown in the bright field (above) and dark field (below) electron micrographs. The sets of fringes in the dark-field image are rotational Moiré fringes, produced by the rotational disorder shown by the arcs in the diffraction pattern (top, right-hand corner).

3.2. THE SULFIDES

The bulk crystalline composition of the series of mixed sulfides determined from XRD powder patterns is given in Table 3, and shown schematically in Fig. 1b. Line broadening due to small crystal size is indicated. The electron microscopy showed that in many cases the surface structure of the crystals was quite different from that in the bulk, so that for catalytic purposes much of this information is irrelevant.

TABLE 3

Crystalline Forms of Sulfide Crystals Identified by XRD

Sample	Composition	Phase present
A	0	MoO_2 sharp
B	30	MoO_2 sharp; MoS_2 trace, broad
C	41	MoO_2 sharp; MoS_2 broad
D	55	MoS_2 broad; NiS_2 sharp, trace
E	73	MoS_2 broad; NIS_2 + NiS, sharp
F	79	MoS_2 broad; NiS + βNi_7S_6, sharp
G	92	MoS_2 trace very broad; NiS + βNi_7S_6, sharp
J	100	Ni_3S_2 sharp

The structure of the sulfides is described below in the same groups of composition range as for the binary oxides, and where possible the morphologies are related to those observed for the oxides.

3.2.1. 100% Mo

The reaction produced single crystals with the bulk structure of MoO_2. Electron diffraction from individual crystals confirmed the XRD results. The crystals frequently took the form of fingers joined as in a hand (Fig. 8a). There were also a few thin sheets of MoS_2 separated from the MoO_2 crystals and frequently extending as a membrane between the fingers. Examples can be seen beyond the edge of the crystal of MoO_2 in Fig. 8a.

High-magnification electron microscopy showed that there were one or two black fringes around the edges of all the crystals in images taken at a slight amount (~500 Å) of underfocus. The behavior of these fringes was quite different from that of the classical Fresnel fringes which are very familiar to electron microscopists. When more than one fringe appeared the spacing was about 6.1 Å. This corresponds to the spacing between adjacent layers of molybdenum atoms in molybdenite. We believe, and hope to justify later, that each black fringe comes from an individual layer of MoS_2, and so we conclude that each MoO_2 crystal is coated with a thin skin of MoS_2, one or a few molecular layers thick, conforming accurately to the outer surface of the MoO_2. Figure 8b shows an electron micrograph taken under conditions for "optimum lattice imaging" of MoO_2 crystals in which there are (100) lattice fringes within the crystals, and two heavier black fringes with a different spacing, surrounding the crystals. Thus, although the bulk structure is MoO_2 the exposed surface of this material consists of a layer of saturated S–S–S atoms such as occurs on the basal plane of MoS_2 crystals.

3.2.2. Mo + O–50% Ni

The components of the original oxide can be clearly recognized because the shapes of the crystals were largely retained after the sulfiding. The MoO_3 was converted to MoO_2, each crystal being coated with a few molecular layers of MoS_2 as described in Section 3.2.1. In addition, there was a component with the morphology of the $NiMoO_4$ (Fig. 9, and compare with Figs. 3, 4). The needles in particular are distinctive. This material gave an electron diffraction pattern of polycrystalline MoS_2 even when individual needles were selected. High-magnification images taken under optimum lattice image conditions contain sets of black fringes with a spacing of about 6.1 Å (Fig. 10). This spacing is consistent with that between the Mo–Mo planes in crystals of MoS_2 (*18*), and similar fringes were formed at the edges of thin flakes of molybdenite. We believe therefore that these sets of fringes come from crystals of MoS_2 viewed roughly edge-on, with

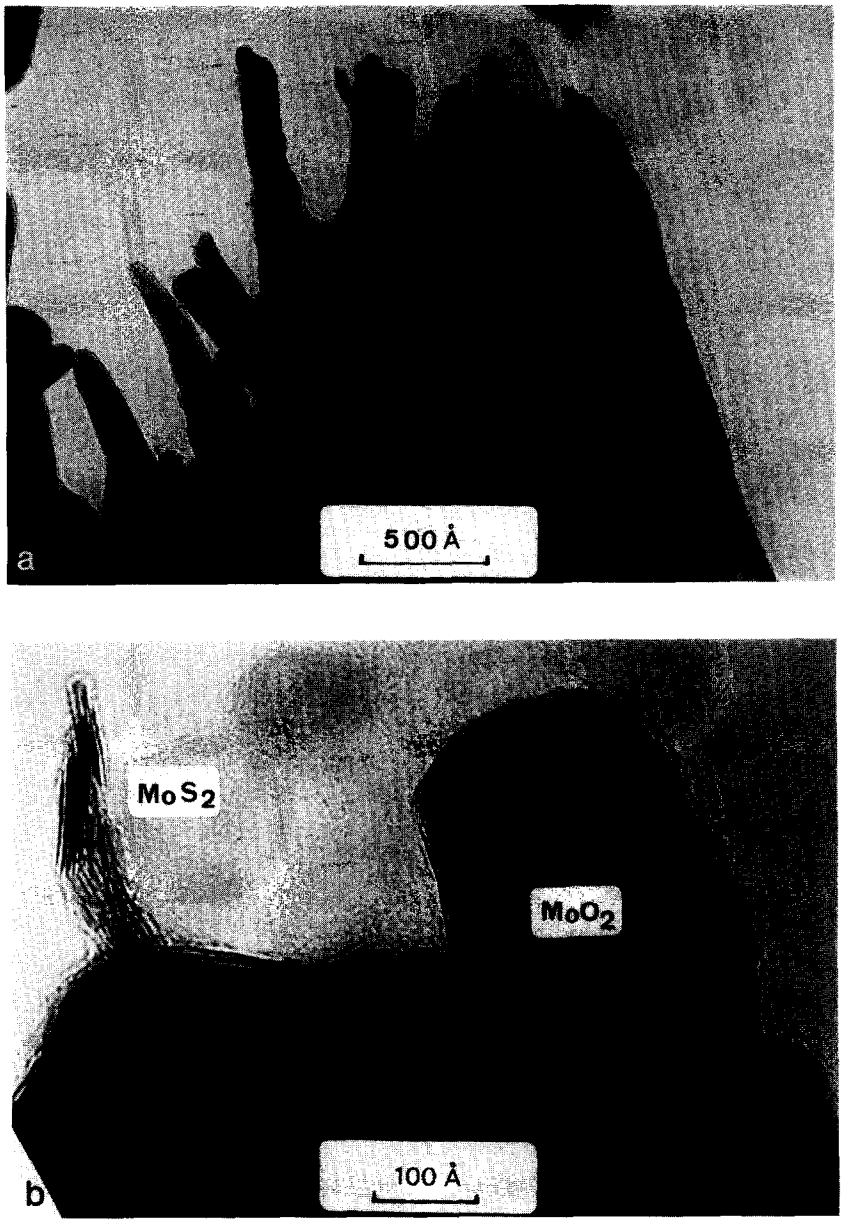

FIG. 8. Electron micrographs of sample A, 100% Mo, after the sulfide treatment and use as a catalyst. (a) "Fingers" of MoO_2 are produced by the reduction of the MoO_3 accompanied by sheets of MoS_2 (right-hand side). (b) At high magnification under lattice image conditions there is a pair of black fringes around each MoO_2 crystal. Some sheets of MoS_2 extend beyond the MoO_2 crystal.

each black line corresponding to a plane of Mo atoms. The contrast of these fringes has been studied in detail, and their through-focus behavior is like that of graphite (*19*), and is in keeping with this interpretation.

These fringes occur in "books" of up to ten fringes, and they are frequently twisted and curved through very small radii of curvature (~100 Å) (Fig. 11). In the needles the fringes tended to be parallel to the long axis; electron diffraction from individual

FIG. 9. The sulfided $NiMoO_4$ retains the morphology of the original oxide crystals. Electron micrograph of sample B sulfided.

needles confirmed this preferred orientation for the MoS_2 crystallites. Otherwise, fringes frequently formed closed loops; in general no regular lattice image could be found in the central region.

Thus it is concluded that the $NiMoO_4$ crystals were converted to highly dispersed MoS_2. There is no crystallographic evidence for the presence of the nickel. There was no evidence in the diffraction patterns for the presence of the phase $NiMo_3S_4$ (*17*).

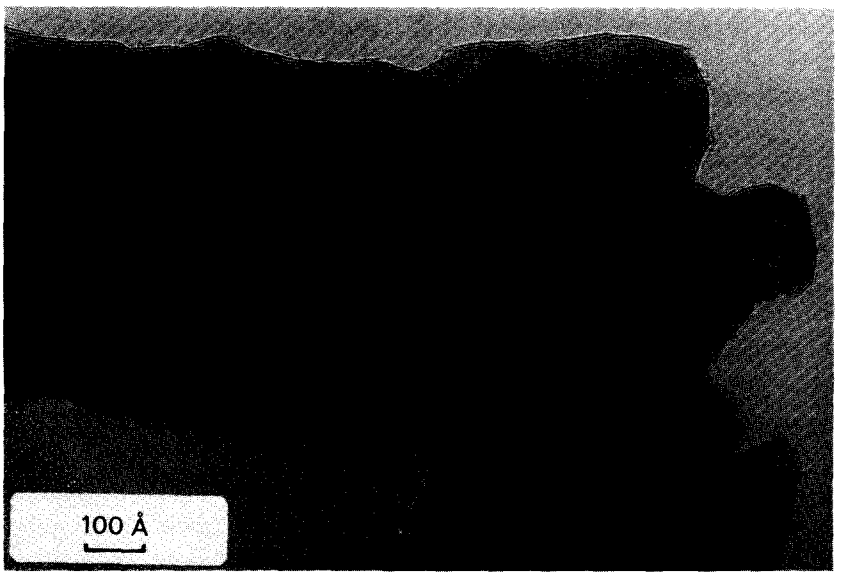

FIG. 10. At higher magnification each needle of the original $NiMoO_4$ is converted by the sulfide treatment to highly dispersed MoS_2. The electron micrograph of sample B shows many books of black fringes with a 6.15-Å spacing, and a set parallel to the surface of the needle.

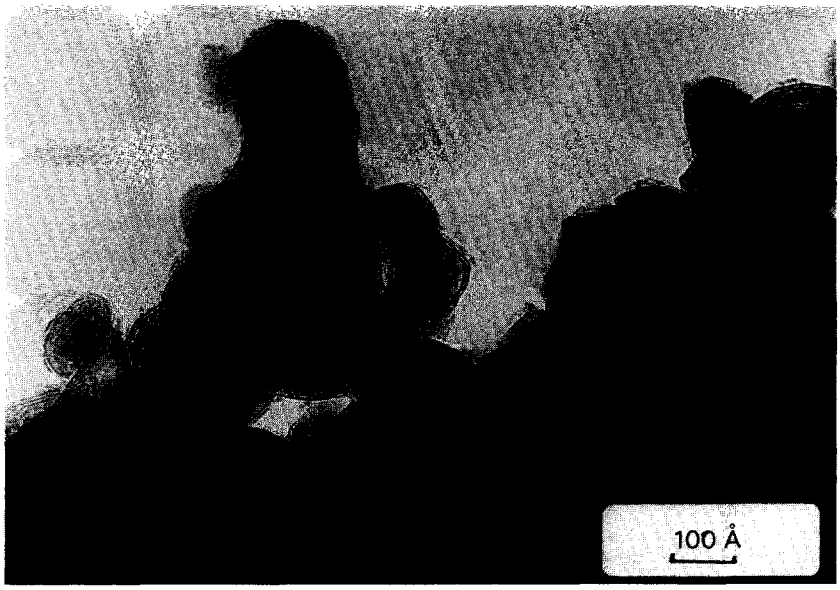

FIG. 11. Electron micrograph of sulfided sample B showing how the small crystals of $NiMoO_4$, C in Fig. 4, are converted to expose a skin of MoS_2, 2 to 10 layers thick.

3.2.3. Mo + 50% Ni

The sample D which is closest to this composition gave an XRD pattern of broad MoS_2 peaks, and two weak (height $<10\%$ that of the 002 peak from MoS_2) additional peaks at 3.26 and 2.85 Å. This XRD pattern is insufficient to identify the phase of nickel sulfide, but it seems likely to be NiS_2. A later reexamination by XRD after some months exposure to air revealed a new series of very weak peaks corresponding to $NiSO_4.2H_2O$.

Electron microscopy and diffraction showed that the MoS_2 was in the highly dispersed form described above (3.2.2.), its overall morphology at lower magnifications conforming to that of the $NiMoO_4$ crystals (3.1.3.). At high magnifications the "books" of MoS_2 containing groups of up to about ten parallel fringes (6.1-Å spacing) were the dominant feature in underfocus images; they are taken to be layers of MoS_2 seen edge-on. It is hoped that this identification will be confirmed by comparison of calculated and observed through-focus series. The flakes of MoS_2 can also be seen normal to the basal plane, and were identified as such by electron diffraction. Their lattice images have very low contrast, but a hexagonal pattern of 2.74-Å spacing (MoS_2 (*18*)) can just be detected in Fig. 12. The edges of these thin flakes are very serrated, as are steps on the surface.

Electron microscopy detected a few isolated crystals of nickel sulfide in quantities about appropriate for the 5% nickel in excess of that accommodated in stoichiometric $NiMoO_4$. Apart from this there is no diffraction evidence for the presence of nickel in this material, even though it must occur in quantities about equal to that of the Mo. Some specimens were therefore examined in a scanning transmission electron microscope (STEM) fitted with an energy-dispersive X-ray analyzer. With the crossover on the specimen adjusted to about 300 Å, typical thin areas were analyzed for Ni, Mo, and S. The system was calibrated with similar samples of pure Ni_3S_2 and MoS_2. The counting accuracy was insufficient to determine the phase of the nickel sulfide present in this specimen. It was concluded from this analysis that

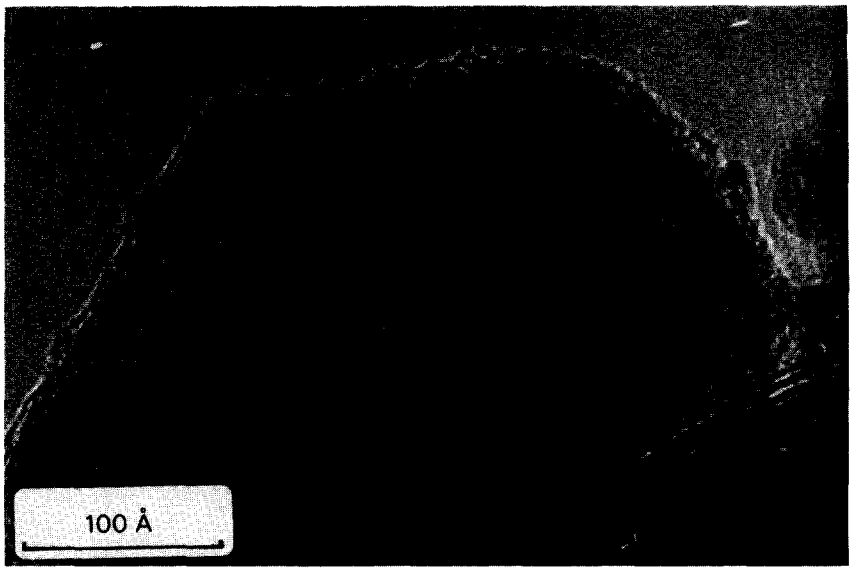

FIG. 12. An electron micrograph of a single flake of MoS_2 from sample D, 55% Ni. It shows a lattice image of the basal projection of the structure (spacing of (100) planes is 2.74 Å), a serrated edge, and steps on the surface of the crystal. Some small crystals seen edge-on at the bottom right-hand corner give the characteristic black fringes (6.15 Å).

apart from a few areas with a relatively high nickel count (probably from a field containing a sulfide crystal) all areas contained nickel distributed in a homogeneous manner at this level of resolution (300 Å).

Thus the $NiMoO_4$ converts to a highly dispersed form of MoS_2 with the external morphology of the original $NiMoO_4$ crystals. The nickel is present within this material in a homogeneous, probably atomically dispersed form.

3.2.4. 50–100% Ni

Table 3 shows that in this composition range a variety of sulfides of nickel were identified in the XRD powder patterns. The MoS_2 pattern became progressively weaker as the proportion of Mo decreased. Electron diffraction from individual crystals confirmed the XRD identification of the nickel sulfides. In addition some as yet unidentified superstructures were observed at higher nickel concentrations. The crystals of nickel sulfide were only a few hundred angstroms in size, in porous clusters, mixed with small flakes of MoS_2, recognized by the "books" of 6-Å fringes (Fig. 13). The nickel sulfide crystals were contained in a skin of MoS_2, shown by a set of 6-Å fringes around the crystals (Fig.14). The number of fringes and hence the thickness of this coating decreased with smaller Mo content. The amount of free MoS_2 also decreased, so that in specimen G (8% Mo), very few free books of MoS_2 occurred (Fig. 14).

In the Mo-free sample, the angular morphology of the NiO crystals was retained, but they have been converted to Ni_3S_2. No black fringes were detected around the edges of these crystals (Fig. 15).

3.3. SUPPORTED CATALYSTS

We have made a preliminary examination at high resolution of Al_2O_3 impregnated with a Ni–Mo solution, calcined at 460°C and then sulfided. Whereas we have been unable to detect any deposit on this surface of the Al_2O_3 immediately after the calcining, we see numerous single or small groups of black lines on the surface after the sulfide treatment. From our experience in examin-

FIG. 13. Electron micrograph of sulfided sample E showing crystals of nickel sulfide and books of MoS_2.

ing the MoS_2 catalysts we believe that these black lines come from individual sheets of MoS_2. Similar features can be seen on commercial catalysts, and Fig. 16 shows a high-magnification electron micrograph of such a catalyst which has been used for hydrogenolysis. It contains single and pairs of black lines which we believe to come from crystalline sheets of MoS_2 in a highly dispersed form.

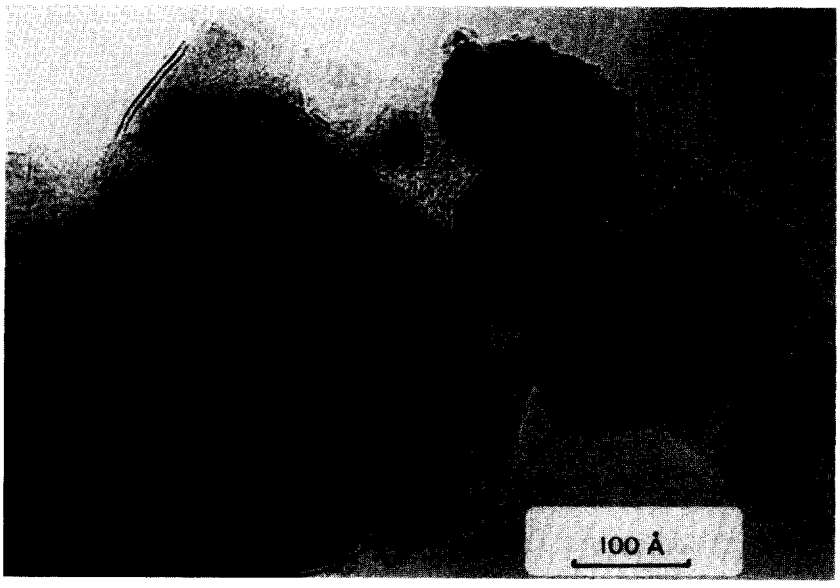

FIG. 14. Electron micrograph of sulfided sample G. The crystals are nickel sulfide, and the black fringes around each crystal show that they are coated with a single or double layer of MoS_2.

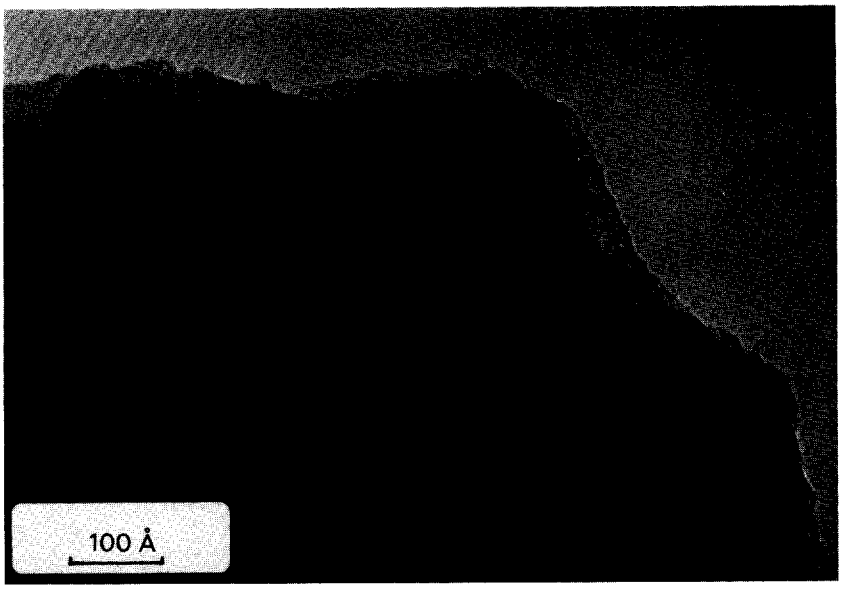

FIG. 15. Electron micrograph of sulfided sample J. In this case there are no black fringes around the edges of the crystal, because the sample contains no Mo (cf. Figs. 8b, 14).

4. DISCUSSION

4.1. THE BINARY OXIDE SYSTEM, Ni + Mo

Our results show that the coprecipitation technique produces well formed crystals of MoO_3,$NiMoO_4$, and NiO for the compositions 100% Mo, 50/50% Ni/Mo, and 100% Ni, respectively. Within the composition range 0–50% Ni a mixture of morphologies

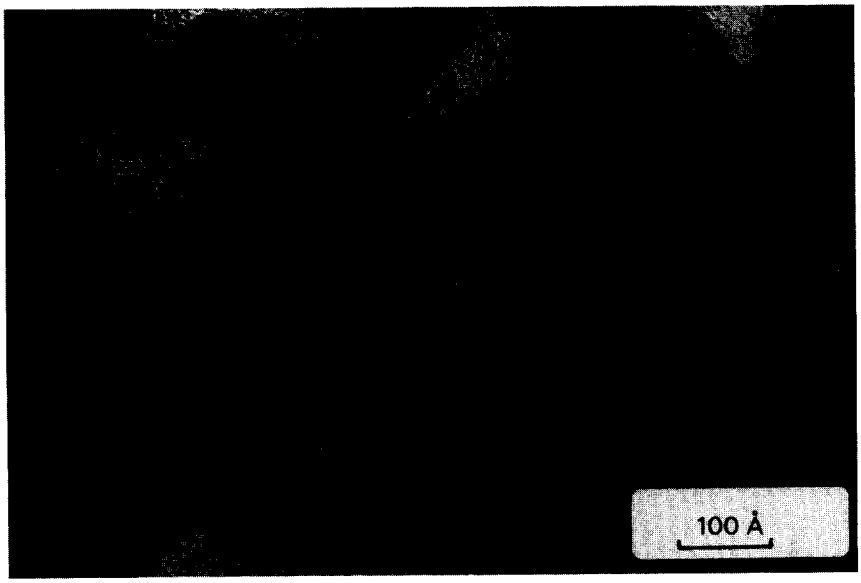

FIG. 16. Electron micrograph of a commercial catalyst which has been used for hydrogenolysis of liquid extracted from coal. We believe that the black lines, about 1 cm long, are lattice images from MoS_2 in sheets one or two layers thick.

of $NiMoO_4$ is produced together with MoO_3. In the range 50–100% Ni the only crystalline phase is NiO, with the Mo incorporated in some manner which in small amounts ($\approx$1%) produces rotational disorder within crystalline plates of NiO. This suggests to us that the Mo is incorporated within the crystal and has segregated in such a fashion as to produce sets of small angle boundaries, stabilized by the presence of the Mo atoms, i.e., the NiO will not tolerate the Mo in solid solution. Larger amounts of Mo produce a highly dispersed, finely crystalline form of NiO. This implies that the Mo is distributed homogeneously on a scale which is too fine to be resolved by electron microscopy, or give its own electron diffraction pattern. These structures seem to be in no way a precursor of the $NiMoO_4$ phase, which seems to form only stoichiometrically, any excess of Ni or Mo being in the form of the respective oxides.

Thus our "phase diagram" is similar to that reported in Ref. (*15*), except that we observe only a small amount of "N-phase" $NiMoO_4$ in sample D (55% Ni), and none in the specimens richer in nickel, contrary to the results in (*15*). We have confirmed that this difference is not due to our lower calcining temperature.

4.2. The Transformation from Oxide to Sulfide

Our microscopy shows that pure MoO_3 is converted only superficially to sulfide, the surface layer being one or two molecular layers thick. One can imagine that this layer is relatively impervious to sulfur atoms, so that the oxide is effectively passivated against further conversion to sulfide. The micrographs show that the layer follows faithfully contours with radii of curvature of 100 Å or less. However, reduction of the core to MoO_2 does occur (by diffusion of H_2 through the sulfide skin), and as a consequence the morphology of the crystals is changed to the "fingers-on-a-hand" type, to account for the 4% density change on reduction.

Very thin sheets of MoS_2 found near and between the fingers, of MoO_2, probably come from a skin of MoS_2 formed initially on the MoO_3 crystals before their reduction and change of shape.

The $NiMoO_4$ converts to a dispersed form of MoS_2. In the needles, the molecular sheets of MoS_2 tend to be parallel to the needle axis, or at least form a surface layer, but on the whole the needles contain a highly discontinuous collection of twisted bundles of MoS_2. Micrographs such as Fig. 11 show the common features of a group of four to six sheets of MoS_2 closed in what must be a roughly spherical form about 100 Å in diameter. It is not clear what is contained within this MoS_2 skin, and electron diffraction shows nothing but a pattern from MoS_2. It seems possible that nickel sulfide in some noncrystalline form remains here, and an X-ray microanalysis shows that the nickel is present homogeneously on this scale. Additionally, MoS_2 occurs mainly in "books" containing a small number of sheets, and only several hundred angstroms in extent.

The nickel sulfides form crystals which are much larger than their precursor oxides. The Mo which was incorporated within the NiO crystals segregates to the surface and forms a skin of MoS_2 on the nickel sulfide crystals or occurs as a separate highly dispersed phase in "books." Qualitatively, it appears as if the nickel sulfides cannot accommodate any Mo in solution.

4.3. Relationship of Structure to Activity

Details of the catalytic activity of these samples are given in Ref. (*13*). The plot of the specific activity against composition was a typical "volcano" curve, with the activity peaking at sample D (55% Ni). Sample E (73% Ni) had the highest surface area (N_2 adsorption), and our electron mi-

croscopy shows that it had a high degree of dispersion of the MoS_2.

The electron micrographs show that samples D and E, the most active catalysts, both contain highly dispersed books of MoS_2, with a very similar structure. However, they were formed from very different forms of oxide; the oxide in D is mostly crystalline stoichiometric $NiMoO_4$, while that in E is very finely crystalline NiO within which Mo is in some way very finely distributed. They share the common feature of having the Ni and Mo coexisting in a homogeneous form, which when sulfided, produces the highly dispersed MoS_2. It is not clear from this study by electron microscopy where the nickel is located and how it has been incorporated. There are several possiblities to be considered:

(i) The Ni is intercalated between the S–S layers of the MoS_2 sheets. Chemical arguments have been made against this proposal (*2, 3*). We have been unable to detect any change in the *c* parameter of the MoS_2 which normally accompanies intercalation (*20*).

(ii) The Ni is accommodated substitutionally within the MoS_2. It is not clear if this would affect lattice images of the basal projection of the MoS_2, but no obvious effect has been detected.

(iii) The Ni is absorbed on the edges of the sheets, and on steps on the surface. Even with the high degree of dispersion produced here, there are insufficient sites to accommodate nickel in this way in amounts equal to the Mo. High-resolution images normal to the flakes of MoS_2 contain only very weak lattice contrast, but show that the edges of the flakes and surface steps are heavily serrated. We have therefore also examined flakes of natural molybdenite, not containing nickel, and they appear to be no less serrated. It is not possible to say therefore that this is an effect of nickel adsorbed on the edges of the MoS_2 layers.

(iv) The Ni exists as a crystalline phase (sulfide). Micrographs do not reveal any such crystals, even in images where 2.7-Å detail appears in lattice images of the MoS_2.

(v) The Ni occurs as a noncrystalline phase perhaps incorporating sulfur, surrounded by MoS_2 layers. Chemical analysis confirms that if all the Mo in the most active catalyst is converted to stoichiometric MoS_2, there is sufficient additional sulfur to form all the nickel into stoichiometric Ni_3S_2 within a few percent (*13*).

The last suggestion seems most likely. It is supported by the observation that after some months of exposure to air, the XRD pattern of sample D showed that its structure had changed, and it now contained an appreciable quantity of crystalline $NiSO_4 \cdot 2H_2O$.

CONCLUSION

Our electron micrographs of supported NiMoS catalysts showed that in the systems we have investigated the MoS_2 exists as single or a small number of molecular sheets highly dispersed on the support, and therefore of a crystalline nature (*21*) rather than as a monolayer on the γ-Al_2O_3 surface (*8, 10*). We believe therefore that the present study is relevant to supported systems and that the support does not play a controlling role in the catalyst activity.

The results for sulfided MoO_3 show that the exposed basal plane of crystalline MoS_2 is not highly active, in the absence of Ni. Furthermore, the basal plane still has a low activity when closely associated with excess Ni, such as in the thin coating of MoS_2 on crystals of nickel sulfide. High activity occurs with high dispersion, the significant change being that the edges of the MoS_2 sheets become exposed. High activity also requires that Ni be associated in some way with this MoS_2, just as for cobalt (*22*). Unfortunately we have been unable to locate the Ni.

We have discussed the various possibilities for the incorporation of the Ni in the MoS_2. In the practical case of promoted MoS_2 on a support, there is no need to consider an intercalation model if in fact the MoS_2 occurs as individually dispersed

sheets (Fig. 16). Because the sheets are about 100 Å wide, and one layer thick, replacement of every edge Mo by Ni requires an atomic proportion of only 6%. We feel that additionally the promoter must be adsorbed on the basal surfaces because proportions much higher than this are required for effective activation.

ACKNOWLEDGMENTS

We wish to acknowledge the helpful assistance of Mr. N. Tamp who prepared specimens, and Mr. H. Jaeger for X-ray diffraction analysis.

REFERENCES

1. Thakur, D. S., Grange, P., and Delmon, B., *J. Less Common Metals* **64**, 201 (1979).
2. Farragher, A. L., and Cossee, P., *in* "Proceedings Fifth International Congress on Catalysis," (J. W. Hightower, Ed.), p. 1301. North-Holland, Amsterdam, 1973.
3. Farragher, A. L., Symposium on the Role of Solid State Chemistry in Catalysis, New Orleans. *Amer. Chem. Soc. Div. Pet. Chem. Prepr.* **22**(2), 524 (1977).
4. Grange, P., and Delmon, B., *J. Less Common Metals* **36**, 353 (1974).
5. Hagenbach, G., Courty, Ph., and Delmon, B., *J. Catal.* **31**, 264 (1973).
6. Wentrcek, P. R., and Wise, H., *J. Catal.* **51**, 80 (1978).
7. Schuit, G. C. A., and Gates, B. C., *AIChE J.* **19**, 417 (1973).
8. Massoth, F. E., "Advances in Catalysis" (D. D. Eley, H. Pines, and P. B. Weisz, Eds.), Vol. 27, p. 266. Academic Press, New York, 1978.
9. Pollack, S. S., Makovsky, L. E., and Brown, F. R., *J. Catal.* **59**, 452 (1979).
10. Massoth, F. E., *J. Catal.* **50**, 190 (1977).
11. Delannay, F., Thakur, D. S., and Delmon, B., *J. Less Common Metals* **63**, 265 (1979).
12. Andrushkevich, M. M., Buyanov, R. A., Sitnikov, V. G., Itenberg, I. Sh., and Khramova, G. A., *Kinet. Catal.* **14**, 464 (1973).
13. Pratt, K. C., Sanders, J. V., and Tamp, N., *J. Cata.* **66**, 82 (1980).
14. Smith, G. W., *Acta Crystallogr.* **15**, 1054 (1962).
15. Plyasova, L. M., Ivanchenko, I. Y., Andrushkevich, M. M., Buyanov, R. A., Itenberg, I. Sh., Khramova, G. A., Karakchiev, L. G., Kustova, G. N., Stepanov, G. A., Tsailingold, A. L., Pilipenko, F. S., *Kinet. Catal.* **14**, 1010 (1973).
16. Pearson, W. B., "Handbook of Lattice Spacings and Structure of Metals and Alloys." Pergamon, Elmsford, N.Y., 1964.
17. Guillevic, J., Bars, O., Grandjean, D., *J. Solid State Chem.* **7**, 158 (1973).
18. Dickinson, R. G., and Pauling, L., *J. Amer. Chem. Soc.* **45**, 1466 (1923).
19. Jefferson, D. A., Millward, G. R., Thomas, J. M., *Acta Crystallogr. A* **32**, 823 (1976).
20. Woollam, J. A., and Somoano, R. B., *Mater. Sci. Eng.* **31**, 289 (1977).
21. de Beer, V. H. J., and Schuit, G. C. A., *in* "Preparation of Catalysts" (B. Delmon, P. A. Jacobs, and G. Ponceclet, Eds.), p. 345. Elsevier, Amsterdam, 1976.
22. de Beer, V. H. J., and Van Sint Fiet, T. H. M., van der Steen, H. A. M., Zwaga, A. C., and Schuit, G. C. A., *J. Catal.* **35**, 297 (1974).